First publ. in: Chemical Physics Letters 301 (1999), 5-6, pp. 546-550

Experimental verification of the high stability of $Al_{13}H$: a building block of a new type of cluster material?

S. Burkart [a], N. Blessing [a], B. Klipp [a], J. Müller [a], G. Ganteför [a,*], G. Seifert [b]

[a] *Fakultät für Physik, Universität Konstanz, D-78457 Konstanz, Germany*
[b] *Institut für Theoretische Physik der TU Dresden, D-01069 Dresden, Germany*

Abstract

Photoelectron spectra of mass-separated, negatively charged, bare and reacted aluminium clusters $Al_nH_m^-$ ($n = 12–14$, $m = 0–2$) are presented and compared to the results of corresponding calculations. A large HOMO–LUMO gap of 1.4 eV is found for the neutral $Al_{13}H$ cluster, indicating an extraordinarily high stability of this cluster. Adsorption of a second hydrogen atom results in the disappearance of the gap.

Since the discovery of fullerenes a new dimension has been added to cluster science: the search for new materials consisting of clusters. However, such materials are metastable and they can only exist, if there is a barrier for reactions with identical clusters and with the substances used in the processes of extraction and separation. Few cluster materials are known at present. Most famous are the various new materials consisting of fullerenes like C_{60} and C_{70} [1]. These clusters are closed-shell species with a relatively large HOMO–LUMO gap (HOMO: highest occupied molecular orbital, LUMO: lowest unoccupied molecular orbital). The most stable species C_{60} has a HOMO–LUMO gap of 1.7 eV, while the gap for the less stable C_{70} is $\sim$ 1.0 eV [2,3]. Generally, the barrier for possible reactions between two neighboring clusters may be correlated with the energy gap between the electronic ground state and the first excited state of a cluster. For a free cluster, this quantity can be derived by anion photoelectron spectroscopy.

Recently, the existence of such materials consisting of metal clusters has been predicted. One such candidate is $Al_{13}K$ [4,5]. The chemical inertness of the Al_{13}^- anion has been demonstrated experimentally [6,7]. This can be explained in terms of the jellium model [8] by the shell completion occurring at 40 electrons (aluminum is trivalent). The neutral Al_{13} cluster is an open-shell species with one electron less than a closed shell. A potassium atom donates one electron to the Al_{13} and, therefore, $Al_{13}K$ has been predicted to be a stable neutral cluster [4,9,10]. Due to the strong charge transfer Al_{13}^- may be viewed as a 'giant ion' and therefore a building block of a hypothetical ionic crystal $K^+Al_{13}^-$ [4].

* Corresponding author. Fax: +49 7531 883091; e-mail: gerd.gantefoer@uni-konstanz.de

Another possible stable cluster might be $Al_{13}H$ [11], if the number of valence electrons is the only parameter relevant for stability. However, hydrogen is much less electropositive than potassium, i.e. the energy of the 1s orbital is below the valence orbitals of aluminum. In contrast to $Al_{13}K$ an electron might be transferred to the hydrogen atom from the Al_{13} cluster forming a H^- ion bound to a positively charged Al_{13}. In such case $Al_{14}H_2$ could be an especially stable species – a 'magic cluster'. Indeed, there are indications that the latter mechanism might be taking place. In a hydrogen chemisorption experiment with Al cations the high stability of $Al_{14}H_1^+$ has been found and explained by the shell closing at 40 electrons [12].

In addition to such ionic contributions one should also take into account a more covalent bonding situation for the interaction of hydrogen with Al_{13}. In this case the formation of deep-lying bound states of the Al_{13} with H would also lead to a stable closed-shell $Al_{13}H$ cluster with a non-zero gap.

To gain more information about the interaction of hydrogen with aluminum clusters, we recorded photoelectron spectra of $Al_nH_m^-$ clusters and performed quantum calculations of Al_nH_m and $Al_nH_m^-$ clusters with $n = 12–14$ and $m = 0–2$.

The Al_n^- clusters were generated using a PACIS (pulsed arc cluster ion source) [13]. Hydrogen gas is introduced into the source resulting in the effective generation of $Al_nH_m^-$ clusters with $n = 2–40$ and $m = 0–2$. The high yield of hydrogen reacted clusters is probably due to the formation of atomic hydrogen in the electric discharge (see, e.g., Ref. [14]). The vibrational temperature of the clusters can be determined from vibrationally resolved photoelectron spectra and is ~ 300 K [13,15]. The anions are mass-separated using a time-of-flight reflectron mass spectrometer. The reflectron is designed for optimum transmission and allows for the focussing of the anion beam into the center of a 'magnetic bottle' time-of-flight electron spectrometer [15]. Under these conditions a mass resolution of $m/\Delta m >$ 350 has been achieved. A selected bunch of clusters is irradiated by a UV-laser pulse and the kinetic energy of the detached electrons is determined from their time-of-flight to the electron detector. The photon energy is 4.66 eV and the pulse energy is kept below 10 mJ/cm^2 to avoid multiphoton processes. The energy resolution of the electron spectrometer is ~ 20 meV.

Fig. 1 shows an expanded view of a time-of-flight mass spectrum of $Al_nH_m^-$ clusters with $n = 12–14$ and $m = 0–2$. No indication of a higher intensity for an even number of adsorbed hydrogen atoms is found supporting the idea of atomic hydrogen generation in the discharge.

Fig. 2 displays a comparison of photoelectron spectra of $Al_nH_m^-$ clusters with $n = 12–14$ and $m = 0–2$. For Al_{13}^-, a single peak (Fig. 2d, marked M) is observed, indicating the high symmetry of this particle [16]. The width of this main peak is ~ 0.4 eV. In addition, the electron affinity of this cluster is rather high compared to the one of Al_{12}^- and Al_{14}^-. Adsorption of a single hydrogen atom alters the spectrum of Al_{13}^- dramatically. A peak at low binding energy (BE) appears (Fig. 2e, marked A), while the main feature (marked M) is slightly broadened (FWHM ~ 0.5 eV) and its position remains unchanged. In addition, a narrow peak (marked X) at high BE appears. Adsorption of a second hydrogen atom results in the disappearance of the peak at low BE (Fig. 2f). The main feature (marked M) exhibits an increased broadening (FWHM ≈ 0.6 eV) and a shoulder at low BE (marked A). The narrow peak at

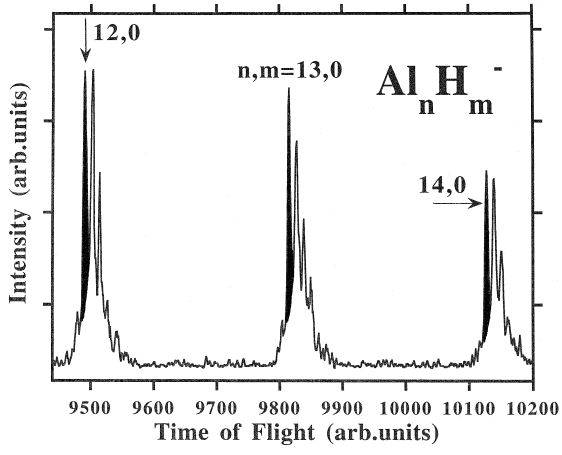

Fig. 1. Expanded view of a time-of-flight mass spectrum of $Al_nH_m^-$ clusters. The largest peaks (black) are assigned to the bare Al_n^- clusters. Mass peaks corresponding to a hydrogen uptake of $m = 1–4$ can be observed. The small peaks at the left-hand shoulders of the peaks assigned to bare Al_n^- clusters are artifacts of the ion detector.

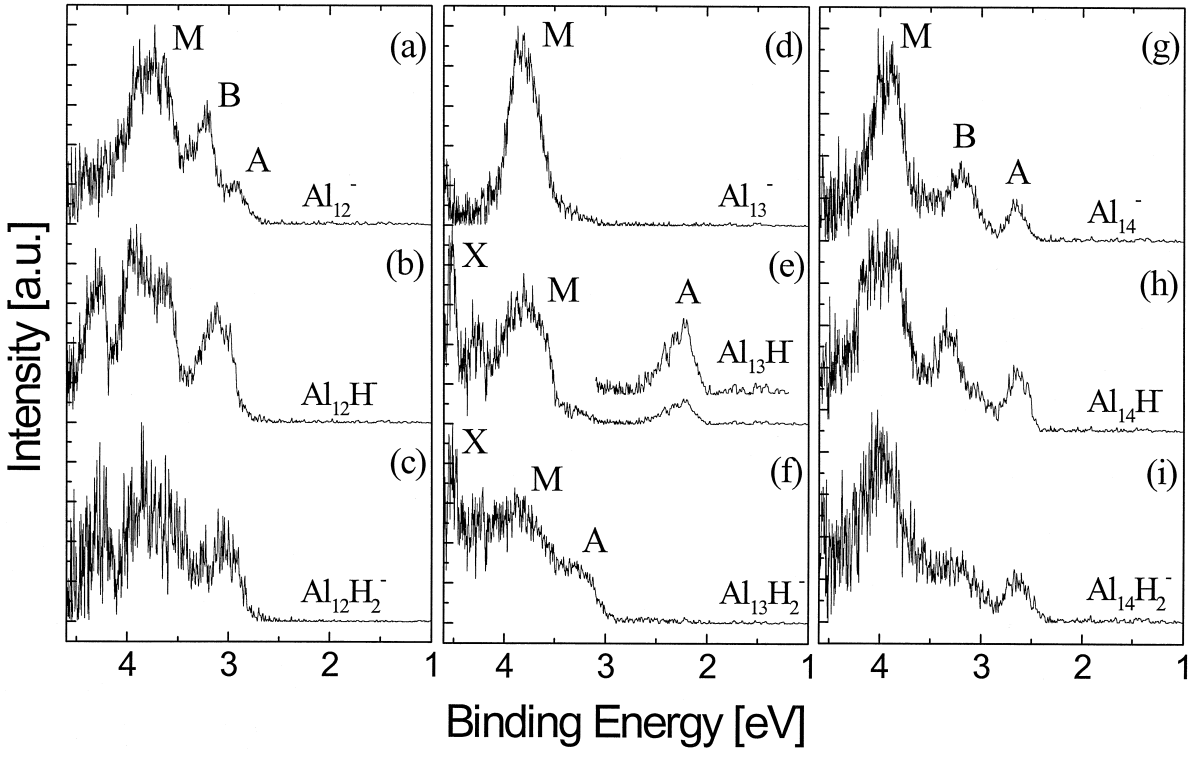

Fig. 2. Photoelectron spectra of bare and reacted $Al_nH_m^-$ cluster anions with $n = 12–14$ and $m = 0–2$. The photon energy is 4.66 eV. For a discussion of the marked features see text.

high BE (marked X) has a similar position and shape as in the spectrum of $Al_{13}H_1^-$.

In the spectra of the neighboring clusters Al_{12}^- and Al_{14}^- the hydrogen induced changes are less obvious. The spectra of the bare clusters exhibit three peaks (Fig. 2a and g, marked A, B, M). The same number of features we observed for the hydrogenated species $Al_{12}H_1^-$, $Al_{12}H_2^-$, $Al_{14}H_1^-$ and $Al_{14}H_2^-$ (Fig. 2b, c, h, i). The positions, shapes and relative intensities show slight variations compared to the spectra of the bare clusters, but no dramatic changes are observed. The electron affinity is almost unchanged by the hydrogen uptake. Comparable, relatively small changes have been found for all other $Al_nH_m^-$ clusters with $n = 2–14$ studied so far [17].

To explain the measured spectra, we performed self-consistent, 'ab initio', density functional calculations for the different clusters. The applied method is an LCAO (linear combination of atomic orbitals) scheme within the local (spin) density approximation (L(S)DA) of density functional theory. We used the code 'adf' (Amsterdam density functional) [18,19], which has the following characteristics: For the wavefunctions an LCAO ansatz was used. The basis set used has triple-zeta quality. All integrals were solved numerically with Gauss–Legendre based integration algorithms, where the space is separated in a special manner. The densities are fitted to a sum of Slater-type functions to simplify the calculation of the multicenter Coulomb integrals.

The close-packed structure of an Al_{13} cluster with the highest average coordination number is an icosahedral one. In the neutral cluster the symmetry is slightly lowered by a Jahn–Teller distortion. The calculated molecular orbital (MO) diagram for Al_{13} is drawn in Fig. 3, which also shows the valence atomic orbitals of Al (3s, 3p); the HOMO is half occupied. The addition of a further electron – leading to Al_{13}^- – stabilizes the perfect icosahedral symmetry and gives a closed-shell system with a gap of

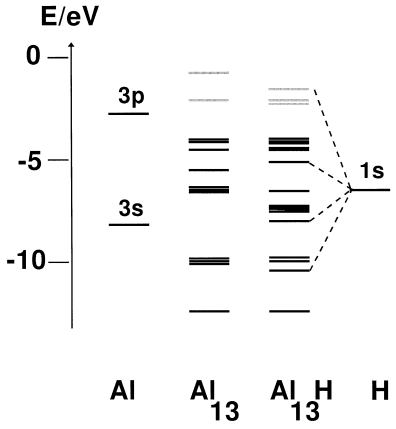

Fig. 3. MO diagrams of neutral Al_{13} and $Al_{13}H$. For comparison the corresponding energies of the atomic valence orbitals (1s H; 3s, 3p Al) are given also. The energies are calculated orbital energies within LDA, which are not directly related to the ionization energies. Dashed lines indicate orbitals of $Al_{13}H$ with large hydrogen contributions, full black bars correspond to occupied orbitals and grey bars to unoccupied ones. The uppermost occupied orbital of Al_{13} is only half occupied.

1.9 eV in agreement with an earlier prediction from Khanna and Jena [11]. The calculated adiabatic ionization energy is 3.6 eV in excellent agreement with the experimental finding (3.5 eV [1], see Fig. 2d).

The addition of a hydrogen atom to the Al_{13} cluster induces only a small disturbance of the high symmetry. The changes in the MO diagram can be seen in Fig. 3 and deep-lying bound states can be identified. Therefore, the hydrogen is strongly bound to the Al_{13} cluster by ~ 3.4 eV (similar to the binding energy calculated by Khanna and Jena [11]). The narrow peak X in the spectrum of $Al_{13}H^-$ (Fig. 2e) might be attributed to the hydrogen induced level ~ 1 eV below the HOMO of $Al_{13}H$ (see Fig. 3).

The bond may be characterized as covalent with an almost neutral hydrogen and deep-lying H–Al_{13} bound states. The HOMO is fully occupied (closed-shell system) with an energy close to that of Al_{13}.

[1] In most cases adiabatic ionization energies cannot be determined from electron spectra. However, the onset of the electron signal al low binding energy can be compared with the calculated adiabatic ionization energy. We determined this onset by fitting a straight line through the steepest part of the slope of the increasing electron signal at threshold and took the intersection of this line with zero as the threshold energy (3.5 eV).

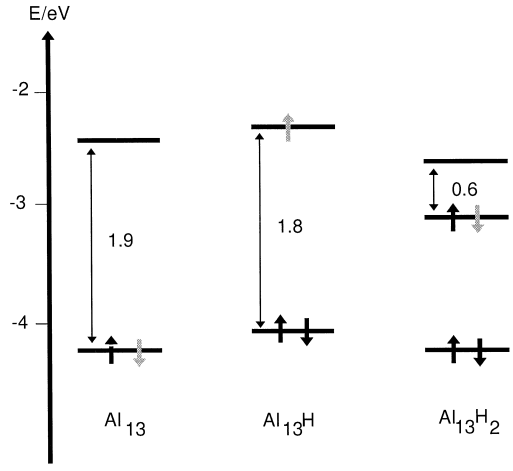

Fig. 4. Calculated HOMOs and LUMOs of Al_{13}, $Al_{13}H$ and $Al_{13}H_2$. The gap energies are given in eV. The occupations of the orbitals are indicated by black and grey arrows for the neutral and the anionic clusters, respectively.

The calculated HOMO–LUMO gap (1.8 eV, see Fig. 4) is nearly as large as that of Al_{13} and roughly corresponds to the energy difference between features A and M in Fig. 2e ($= 1.4 \pm 0.2$ eV). The additional electron in $Al_{13}H^-$ has to occupy this LUMO. Photoemission from the singly occupied LUMO gives rise to the appearance of a small peak at low BE (Fig. 2e, marked A). The low intensity of the peak corresponds to an occupation number of

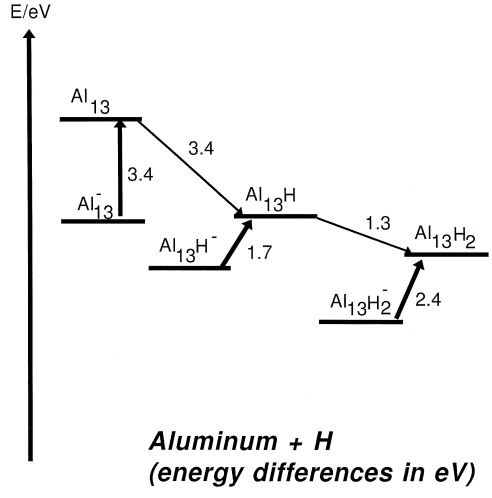

Fig. 5. Calculated energy diagrams for Al_{13}, $Al_{13}H$, $Al_{13}H_2$ and the corresponding anions. Energy differences are given in eV.

one compared to the main peak (Fig. 2e, marked M) which corresponds to a manifold of energy levels around −4 eV BE (Fig. 3). The calculated (adiabatic) and the measured ionization energies of $Al_{13}H^-$ of 1.7 eV (see Fig. 5) and 2.0 eV (see Fig. 2e) respectively confirm this assignment of the HOMO–LUMO gap of the neutral $Al_{13}H$ cluster.

A second hydrogen atom can be bound to the Al_{13} cluster. However, the binding energy is only 1.3 eV (Fig. 5) and considerably smaller than that of the first one indicating saturation. Like Al_{13}, the $Al_{13}H_2$ cluster has a half occupied HOMO (Fig. 4). The addition of a further electron fills this orbital giving a closed-shell system similar to Al_{13}^-. This explains why the photoelectron spectrum of $Al_{13}H_2^-$ (Fig. 2f) looks similar to that of Al_{13}^- (Fig. 2d) and why no remarkable gap can be seen. The low binding energy of the HOMO in $Al_{13}H_2$ indicates a smaller ionization energy of $Al_{13}H_2^-$ compared to that of Al_{13}^-. The calculated (adiabatic) ionization energy (2.4 eV, see Fig. 5) of $Al_{13}H_2^-$ is 0.7 eV higher than that of $Al_{13}H^-$. A similar shift of the ionization energies is observed in the spectra (1 eV), going from $Al_{13}H$ to $Al_{13}H_2$ (see Fig. 2f).

In conclusion, we present photoelectron spectra and LDA calculations of bare and reacted $Al_nH_m^-$ clusters. The spectrum of $Al_{13}H^-$ indicates an extremely large HOMO–LUMO gap of 1.5 eV is the neutral cluster in agreement with the calculations. The icosahedral symmetry of the Al_{13}^- anion is only slightly disturbed by the hydrogen adsorption. In contrast, the $Al_{13}H_2^-$ cluster is a rather unstable open-shell species with a much smaller HOMO–LUMO gap. All other Al_nH_m clusters studied so far have similar small HOMO–LUMO gaps [17]. The large gap makes the $Al_{13}H$ cluster a promising candidate as a building block for cluster materials analogous to C_{60}.

Acknowledgements

We thank D. Kreisle, E. Recknagel and W. Eberhardt for their support. The additional support of the Deutsche Forschungsgemeinschaft is acknowledged.

References

[1] W. Krätschmer, L.D. Lamb, K. Fostiropoulos, D.R. Huffman, Nature (London) 347 (1990) 354.
[2] S.H. Yang, C.L. Pettiette, J. Conceicao, O. Cheshnovsky, R.E. Smalley, Chem. Phys. Lett. 139 (1987) 233.
[3] H. Handschuh, G. Ganteför, B. Kessler, P.S. Bechthold, W. Eberhardt, Phys. Rev. Lett. 74 (1995) 1095.
[4] S.N. Khanna, P. Jena, Chem. Phys. Lett. 219 (1994) 479.
[5] F. Liu, M. Mostoller, Th. Kaplan, S.N. Khanna, P. Jena, Chem. Phys. Lett. 248 (1996) 213.
[6] R.E. Leuchtner, A.C. Harms, A.W. Castleman, J. Chem. Phys. 91 (1989) 2753.
[7] R.E. Leuchtner, A.C. Harms, A.W. Castleman, J. Chem. Phys. 94 (1991) 1093.
[8] W.A. de Heer, Rev. Mod. Phys. 65 (1993) 611.
[9] A. Nakajima, K. Hoshino, T. Naganuma, Y. Sone, K. Kaya, J. Chem. Phys. 95 (1991) 7061.
[10] K. Hoshino, K. Watanabe, Y. Konishi, T. Taguwa, A. Nakajima, K. Kaya, Chem. Phys. Lett. 231 (1994) 499.
[11] S.N. Khanna, P. Jena, Chem. Phys. Lett. 218 (1993) 383.
[12] M.F. Jarrold, J.E. Bowers, J. Am. Chem. Soc. 110 (1988) 70.
[13] C.-Y. Cha, G. Ganteför, W. Eberhardt, Rev. Sci. Instrum. 63 (1992) 5661.
[14] J. Paul, Phys. Rev. B 37 (1988) 6164.
[15] H. Handschuh, G. Ganteför, W. Eberhardt, Rev. Sci. Instrum. 66 (1995) 3838.
[16] C.-Y. Cha, G. Ganteför, W. Eberhardt, J. Chem. Phys. 100 (1994) 1.
[17] P. Jena, B. Rao, S. Burkart, N. Blessing, G. Ganteför, G. Seifert (to be published).
[18] P.M. Boerrigter, G. te Velde, E.J. Baerends, Int. J. Quantum Chem. 33 (1988) 87.
[19] G. te Velde, E.J. Baerends, J. Comput. Phys. 99 (1992) 84, and references therein.